

# Accepted Manuscript

Frost heave in freezing soils: A quasi-static model for ice lens growth

Yukun Ji, Guoqing Zhou, Yang Zhou, Veerle Vandeginste



PII: S0165-232X(18)30232-5  
DOI: <https://doi.org/10.1016/j.coldregions.2018.11.003>  
Reference: COLTEC 2687  
To appear in: *Cold Regions Science and Technology*  
Received date: 18 May 2018  
Revised date: 29 October 2018  
Accepted date: 5 November 2018

Please cite this article as: Yukun Ji, Guoqing Zhou, Yang Zhou, Veerle Vandeginste , Frost heave in freezing soils: A quasi-static model for ice lens growth. Coltec (2018), <https://doi.org/10.1016/j.coldregions.2018.11.003>

This is a PDF file of an unedited manuscript that has been accepted for publication. As a service to our customers we are providing this early version of the manuscript. The manuscript will undergo copyediting, typesetting, and review of the resulting proof before it is published in its final form. Please note that during the production process errors may be discovered which could affect the content, and all legal disclaimers that apply to the journal pertain.

# Frost heave in freezing soils: A quasi-static model for ice lens growth

Yukun Ji <sup>a, b</sup>, Guoqing Zhou <sup>a, \*</sup>, Yang Zhou <sup>a</sup>, Veerle Vandeginste <sup>b, c</sup>

<sup>a</sup> State Key Laboratory for Geomechanics and Deep Underground Engineering, China University of Mining and Technology, Xuzhou, Jiangsu, 221116, China

<sup>b</sup> GeoEnergy Research Centre, Faculty of Engineering, University of Nottingham, Nottingham, NG7 2RD, UK

<sup>c</sup> School of Chemistry, University of Nottingham, Nottingham, NG7 2RD, UK

**Abstract:** Frost heave can have a very destructive impact on infrastructure in permafrost regions. The complexity of nanoscale ice-mineral interactions and their relation to the macroscale frost heave phenomenon make ice lens growth modelling an interesting but challenging task. Taking into account the limiting assumption of the constant segregation temperature in the segregation potential model, we propose here a new quasi-static model for ice lens growth under a time varying temperature based on the water activity criterion. In this model, the conventional pressure potential gradient in Darcy's law is replaced by a water activity based chemical potential gradient for the calculation of water flow velocity, which provides a better prediction of ice lens growth and is useful to describe the ice nucleation and the state of water at a specific temperature. Moreover, based on the analysis of the new developed model, a mathematical description of the segregation potential is provided here. The modified Kozeny-Carman equation is applied to determine the water permeability of a given soil. In our new model, the effects of the equivalent water pressure are taken into account to modify the freezing characteristic function. Hence, the temperature- and equivalent water pressure- dependent hydraulic permeability in the frozen fringe is mathematically determined and improved. By coupling the quasi-static model with the modified hydraulic permeability function, the numerical calculation of ice lens growth is validated based on the experimental data of the temperature of the ice lens measured in the laboratory. The prediction of ice lens growth using the proposed method contributes and facilitates the simplified calculation of frost heave in the field and/or laboratory scenarios at a quasi-static state, and thus enables a better understanding of phase change and fluid flow in partially frozen granular media (soils).

**Keywords:** Water activity; Quasi-static process; Kozeny-Carman equation; Phase change; Nucleation.

## 1 Introduction

Frost heave in cold regions causes significant damage to infrastructure such as railways, pipelines, and buildings (Palmer and Williams, 2003; Zhang et al., 2014; Li et al., 2017). This phenomenon, which has been described not only on Earth, but also on Mars (Sizemore et al., 2015), is mainly caused by the initiation and growth of ice lenses during freezing. The underlying physicochemical mechanisms involve molecular interactions at interfacial contacts, fundamental in our understanding of a wide range of processes of crystallization, nucleation, phase changes, and mineral replacement. When a freezing front propagates in fine-grained granular media, the unfrozen liquid films are absorbed onto particle surfaces and remain in their liquid state in equilibrium at temperatures that are below the freezing temperature (Dash et al., 1995). Premelting dynamics reveals that long-range intermolecular forces will drive

the external water to the freezing front (Rempel et al., 2004), which feeds the accumulation of ice particles and results in the formation of a horizontal soil-free ice lens and frost heave (Rempel, 2007; Sheng et al., 2013; Lai et al., 2014; Zhou and Zhou, 2012; Ji et al., 2018). Mass transfer via water migration is a key mechanism during frost heaving (Konrad and Morgenstern, 1982; Woster and Wettlaufer, 1999; Zhou and Li, 2012; Ji et al., 2017). Accurate prediction of ice lens growth is critical in the stability assessment of construction engineering in cold regions since frost heave mainly results from the growth of an ice lens associated with water flow in the frozen fringe.

In recent decades, research on the coupled thermal-hydro-mechanical (THM) theory has gained increasing attention in the development of frost heave models. Depending on the application, frost heave models have been established with differing types. Generally, mathematical models for the freezing process can be classified into: (i) the mechanistic frost heave model (Gilpin, 1980; O'Neil and Miller, 1985; Nixon, 1991; Rempel et al., 2004; Michalowski and Zhu, 2006; Lai et al., 2017), (ii) the physical field model (Harlan, 1973; Fremond and Mikkola, 1991; Zhang et al., 2016), and (iii) the growth model of a single ice lens (Konrad and Morgenstern, 1980, 1981). For the theoretical models of the frozen soil, some governing equations are necessarily solved, either in coupled or uncoupled ways, and some material parameters must be included, depending upon the complexity and the accuracy of the model itself. Moreover, the physical field models focus on the prediction of the moisture field, mechanical field, and temperature field. The mechanistic frost heave models explain the mechanism of frost heave and describe the evolvement of the ice lenses in freezing soil.

The segregation potential model, which was first proposed by Konrad and Morgenstern (1980), is a typical growth model of a single ice lens. The simplified model is established based on frost heave characteristics near thermal steady state. The segregation potential model indicates that water flux is proportional to thermal gradient in the frozen fringe. Furthermore, the proportionality is defined as the segregation potential. Previous studies have demonstrated the applicability of the model to predict frost heave in the field and under laboratory conditions (Nixon, 1982; Konrad and Shen, 1996; Tiedje and Guo, 2012).

In most laboratory and field scenarios, external water continuously migrates into the frozen fringe after the active zone (Fig. 1) reaches a thermal steady state, and significant growth of the ice lens can then be observed. Hence, upon the evaluation of the limitation of the segregation potential model in this paper, we develop a water activity based quasi-static model for ice lens growth, and assume liquid flow is driven by a chemical potential gradient. The modified Kozeny-Carman equation is applied to determine the water permeability of a given soil. Additionally, the effect of matrix particles on modifying the phase behavior of pore water is taken into account. In fine-grained granular media, the high surface curvature induced by small pore sizes and particles causes decreases in the phase change temperature

(Scherer, 1999). Moreover, in our new model, the equivalent water pressure is taken into account to determine the unfrozen water content. Subsequently, the temperature- and equivalent water pressure- dependent hydraulic permeability in the frozen fringe is then mathematically determined and improved. By coupling the quasi-static model with the modified hydraulic permeability function, a quantitative evaluation of frost heave is performed by examining the process of ice lens growth using experimental data of the temperature of an ice lens measured in the laboratory. The observed consistency between the numerical and experimental results validates the new model.

## 2 The segregation potential model

The assumptions made in the segregation potential model (Konrad and Morgenstern, 1980) are as follows: (i) the thermal permeability is a constant in the frozen fringe, the difference of thermal permeability in the frozen fringe and unfrozen zone is negligible since the segregation temperature is close to the freezing temperature, Akagawa (1988) has proven the validity of this assumption; (ii) after the onset of formation of the warmest ice lens, i.e. near thermal steady state, the particular segregation temperature  $T_s$ , and the overall hydraulic permeability  $\bar{k}_f$  are both a constant.

The analysis above shows, that the growth of warmest ice lens and the water intake flux  $V$ , is proportional to the thermal gradient  $\text{grad}T$  in the frozen fringe. This proportionality is defined as the segregation potential  $SP$ , and the velocity of water flow can be written as follows:

$$V = SP \cdot \text{grad}T \quad (1)$$

The segregation potential theory indicates that water flow is continuous across the frozen fringe at steady-state condition. However, as discussed more below, the segregation temperature is not a constant, it varies with time during freezing, which will further affect the segregation potential and water flow velocity. Hence, the steady-state based solution for the growth of ice lens limits the application of this model. Hence, further research is required to obtain a better understanding of the growth of an ice lens during unsteady-state freezing.

## 3 A water activity based quasi-static model for the growth of ice lens

### 3.1 Governing equations describing the growth of a single ice lens

After the appearance of the warmest ice lens, the soil column is distinguished into two zones near the warm end of the ice lens (Fig. 1), i.e. the passive zone ( $x > x_s$ ) and the active zone ( $x < x_s$ ). The zone for the frozen fringe is between the warm side of the active ice lens and the freezing front ( $x = x_f$ ).

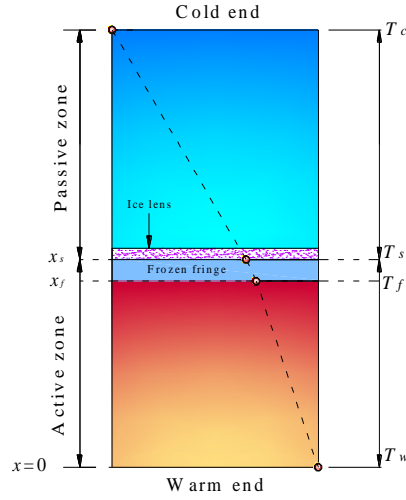


**Fig. 1.** Schematic of soil column after the appearance of the warmest ice lens.

$T_c$ ,  $T_w$ ,  $T_s$ , and  $T_f$  shown in Fig. 1 represent the cold end temperature, the warm end temperature, the temperature of the ice lens, and the freezing temperature respectively. The active zone experiences a coupled process of heat and mass transfer during freezing. The active zone reaches a thermal steady state rapidly due to the slow variation of temperature of the ice lens. Therefore, we assume that the active zone experiences a quasi-static process during freezing.

The heat transport equation in the active zone can be written as follows:

$$\nabla(\lambda \nabla T) - c_w \rho_w \nabla(v_x T) = \frac{\partial(\bar{c}_\rho T)}{\partial t} \quad (2)$$

where  $\lambda$ ,  $v_x$ , and  $\bar{c}_\rho$  are thermal permeability, fluid flow velocity in  $x$ -direction, and volumetric specific heat capacity;  $c_w$ , and  $\rho_w$  stand for bulk specific heat capacity and density of water respectively.

The thermal convection at the left-hand side of Eq. (2) is very small, and it is generally negligible (Nixon, 1991). Based on the assumption of a quasi-static state for the active zone, the term on the right-hand side is negligible. Thus, the heat transport equation can be simplified:

$$\nabla(\lambda \nabla T) = 0 \quad (3)$$

The boundary conditions for the active zone can be written as:

$$\begin{cases} x = 0 : T = T_w \\ x = x_s : T = T_s(t) \end{cases} \quad (4)$$

From Eq. (3) and (4), it can be found that the temperature field in the active zone is entirely determined by the temperature of the ice lens  $T_s$ . In addition, the frozen fringe thickness  $a$ , is also determined by the temperature of the ice lens since the freezing temperature can be considered as a constant value.

Koop et al. (2000) suggested that the kinetic process of ice nucleation is dominated entirely by water activity and

reported the ‘water activity criterion’ for homogeneous ice nucleation. Subsequently, the heterogeneous ice freezing experiments were conducted by Zobrist et al. (2008), and the results strongly suggest that the water activity criterion is also applicable to heterogeneous ice nucleation. Wu et al. (2015) regarded the water activity  $a_w$  as an inducing factor for ice-water phase change, which is a function of temperature:

$$\ln a_w = -\left(\frac{\Delta_m H_1(T_a) - \Delta c_p T_a}{R}\right)\left(\frac{1}{T} - \frac{1}{T_a}\right) - \frac{\Delta c_p \ln(T_a / T)}{R} \quad (5)$$

where  $T_a$  represents the freezing temperature of pure bulk water, i.e.  $T_a=273.15\text{K}$ ,  $\Delta_m H_1(T_a)$  is the molar latent heat at the freezing temperature, and  $\Delta c_p$  stands for the difference in specific heat capacity between water and ice:

$$\Delta c_p = c_{p,\text{liq}} - c_{p,\text{solid}} \quad (6)$$

It can be seen from Eq. (5) that the water activity of pure bulk water equals 1 ( $a_w=1$ ) when the temperature  $T=T_a$ , at which ice and water coexist in equilibrium. However, under the influence of capillarity, the water activity in pore water is different from that in pure bulk water.

The surface tension at internal surfaces of the matrix increases when the ice is generated. With decreasing pore radius, the freezing temperature of condensed water is increasingly depressed. Accordingly, the freezing point for a crystal formed in porous media differs from that of a large flat crystal (Scherer, 1999):

$$\Delta T_f^* = \frac{\sigma_{iw} \kappa_{iw}}{\Delta S_{fv}} \quad (7)$$

where  $\sigma_{iw}$  represents the energy of the ice-water interface, and  $\sigma_{iw}$  is estimated to be  $0.04 \text{ J/m}^2$ ; and  $\Delta S_{fv}$  is the entropy of fusion per unit volume of crystal,  $\Delta S_{fv}=1.2 \text{ J}/(\text{cm}^3\text{K})$ . Ice penetrates into pores of the fine-grained granular media when the curvature of the ice-water interface  $\kappa_{iw}$  is greater than the  $2/r_p$ , where  $r_p$  is the characteristic radius of the pore throats between pores. In this paper, we consider that the curvature of the ice-water interface  $\kappa_{iw}$ , is close to the curvature of the soil grain surface since the liquid film around the soil grain is thin. Thus the interval average is applied to approximately determine the curvature:

$$\kappa_{iw} = -\int_0^\infty m(r) dr / r \quad (8)$$

where  $m(r)$  is the mass fraction of the soil grain with the radius in  $(r, r+dr)$ . This indicates that smaller particles and pore sizes result in high curvature and further lead to depression of the phase change temperature.

Consequently, the phase transition temperature  $T_f$  can be expressed by considering the effect of pore structure on the freezing point:

$$T_f = T_a + \Delta T_f^* \quad (9)$$

It can be found from Eq. (9) that the phase transition temperature is affected by matrix particles. Moreover, with considering the capillarity effect, when ice and water coexist in equilibrium in granular media,  $a_w < 1$ ,  $T_f < T_a$ .

Based on the definition of the water activity criterion, the chemical potential of the water under a given temperature can be determined as follows:

$$\mu_w = \mu_{w,0} + RT \ln a_w \quad (10)$$

where  $\mu_{w,0}$  represents the chemical potential of pure water at the temperature  $T$ , and  $R$  stands for the universal gas constant.

The liquid motion is driven by a thermal gradient which results in a chemical potential gradient, driving water from the place with high chemical potential to the place with low chemical potential (from high temperature to low temperature). Wu et al. (2015) deduced and defined a new concept for water flow velocity in unit volume in granular media based on the thermodynamic theory:

$$V = -n S_w M \frac{1}{V_{m,w}} \nabla \mu_w \quad (11)$$

where  $n$  is porosity,  $S_w$  stands for the saturation degree of water,  $M$  represents the migration rate under unit driving force, and  $V_{m,w}$  is the molar volume of water.

In the active zone, the water flow can still be considered as Darcy flow dominated by equivalent water pressure (negative pressure), and the pressure gradient determined water flow velocity can be presented by (Zhou and Zhou, 2012; Ji et al., 2018):

$$V = -k_f \nabla P \quad (12)$$

Moreover, the driving forces induced by the pressure gradient  $\nabla P$  and chemical potential gradient  $\nabla \mu_w / V_{m,w}$  are equal for the unit volume water. Therefore, the coefficient  $n S_w M$  in Eq. (11) and the coefficient  $k_f$  in Eq. (12) are equal. Importantly, it should be noted that an upward flow occurs only when the driving force in liquid water exceeds the gravity. Consequently, considering the effect of gravity, the average water flow velocity in granular media can be written as:

$$V = -k_f \left( \frac{1}{V_{m,w}} \nabla \mu_w + \rho_w g \nabla x \right) \quad (13)$$

## 3.2 Estimation of hydraulic permeability

### 3.2.1 Hydraulic permeability for a given soil

The hydraulic permeability is a critical parameter governing water flux and fluid flow in the active zone, and a key

aspect to predict ice lens growth in freezing soil. Hydraulic permeability appears to vary in different soil types due to the different specific area, grain size distribution, particle shape etc. A good estimation of hydraulic permeability in different soil types is necessary for numerical simulation of frost heave, and numerous researchers have reported different expressions for hydraulic permeability in soils (Kozeny, 1927; Carman, 1937; Tarnawski and Wagner, 1996; Roque and Didier, 2006; Sante et al., 2015). The most accepted equation is the classical Kozeny-Carman relation (Kozeny, 1927; Carman, 1937), which is known for its accurate prediction to describe the hydraulic permeability in coarse-grained granular media such as sands:

$$k = C \frac{e^3}{1 + e} \quad (14)$$

where  $C$  stands for a coefficient of soil fineness, type, and shape;  $e$  is the void ratio of soil.

In order to overcome the limitation of Eq. (14) for application to fine-grained soil, Ren et al. (2016) reported a modified Kozeny-Carman equation with consideration of the Poiseuille's law and the concept of effective void ratio. This latter method describes more accurately the observed hydraulic permeability in a wide range of soils, from fine-grained to coarse-grained soil. The mathematical description of the modified Kozeny-Carman is expressed by Eq. (15), which establishes the relationship between  $k$  and specific surface area  $S$ . In the special case where  $m=0$ , the equation transforms to Kozeny-Carman relation in Eq. (14). The best fitted parameters  $m$  for sand, silt and clay are  $0 \pm 0.1$ ,  $1.0 \pm 0.2$  and  $1.5 \pm 0.5$ .

$$k = C \frac{e^{3m+3}}{(1+e)^{\frac{5}{3}m+1} [(1+e)^{m+1} - e^{m+1}]^{\frac{4}{3}}} \quad (15)$$

$$C = 2.94 \times 10^{-4} S^{-1.45} \quad (16)$$

Based on the modeling of Eq. (15), it can be found that the hydraulic permeability decreases as specific surface area increases (Fig. 2). Soil particles with the smaller specific surface area are more favorable for water to flow. In addition, hydraulic permeability is largest in sand, followed by silt and then clay, considering the same specific surface area.

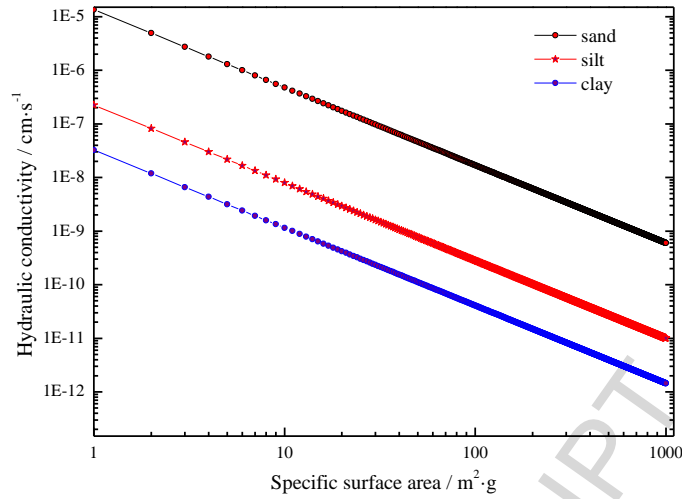


**Fig. 2.** The relationship between hydraulic permeability and specific surface area (void ratio=0.4).

In order to completely describe the hydraulic permeability for a given soil, the mathematics expression of specific surface area should be provided. The specific surface area is related to the shape and the size of soil grains, Sun (2014) proposed a relationship between specific surface area  $S$  and geometric mean diameter  $d_g$  (Tarnawski and Wagner, 1996):

$$S = 1.07 \times d_g^{-0.901} \quad (17)$$

$$d_g = \exp(m_{sa} \ln d_{sa} + m_{si} \ln d_{si} + m_{cl} \ln d_{cl}) \quad (18)$$

where  $m_{sa}$ ,  $m_{si}$ , and  $m_{cl}$  are sand, silt, and clay mass fractions, respectively;  $d_{sa}$ ,  $d_{si}$ , and  $d_{cl}$  are the particle size limits separating sand, silt, and clay respectively.

The specific surface area is small in soils where the mass fraction of clay in the soil is less than 0.25 (Fig. 3). However, the specific surface area increases significantly with increasing mass fraction of clay in the soil, and thus it decreases the hydraulic permeability. Similarly, the specific surface area of the soil increases as silt increases when similar mass fractions of clay are considered.

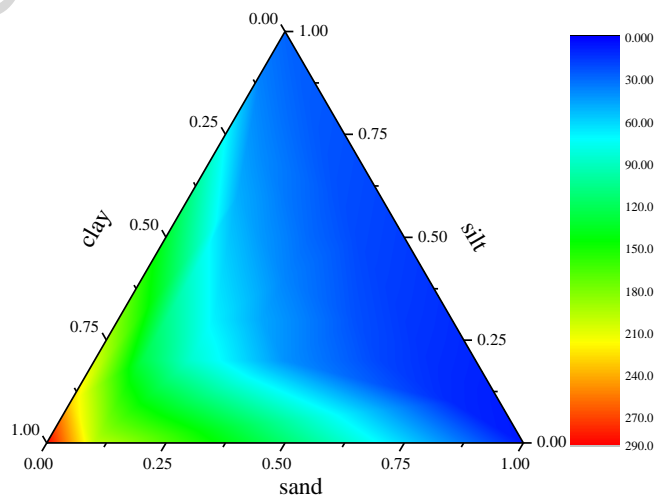


**Fig. 3.** The specific surface area of different soil types.

The soil in nature can be regarded as a mixture of sand, silt, and clay. By combining the different hydraulic permeability of different soil types with the same specific surface area, the hydraulic permeability can thus be determined for a given soil.

### 3.2.2 Unfrozen water content influenced hydraulic permeability in the frozen fringe

Eqs. (15) to (18) constitute the governing equations for the calculation of the hydraulic permeability of a given soil. However, the permeability in the frozen fringe is completely different from that in the unfrozen soil. Loch and Miller (1975) estimated that the frozen fringe thickness is about 4~4.5 mm, whereas Konrad and Morgenstern (1981) reported the measurements of about 1.5~2.7 mm. Unfrozen pore water and ice coexist in the frozen fringe (Fig. 4). Due to the existence of pore ice, the interconnected unfrozen pore water provides the fluid conduits for the water flow from the unfrozen zone to the warmest ice lens. Importantly, the decrease of unfrozen pore water (i.e. increase of pore ice) decreases the seepage pathways, blocking the migration of water and affecting the hydraulic permeability in the frozen fringe.

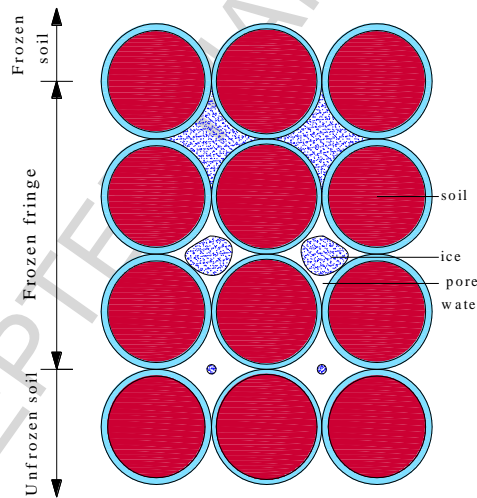


**Fig. 4.** Schematic diagram of the frozen fringe.

As a consequence, the hydraulic permeability is affected mainly by the unfrozen water in the frozen fringe. Anderson and Tice (1972) proposed a well-established power function to describe the relationship between the unfrozen water and temperature:

$$w_u = A(-T)^B, \quad \theta_u = \frac{\rho_d}{\rho_w} A(-T)^B \quad (19)$$

where  $w_u$  is the gravimetric unfrozen water content,  $\theta_u$  is the volumetric unfrozen water content;  $A$  and  $B$  are the soil parameters, and Nixon (1991) suggested that  $A=0.0038S^{0.851}$ ,  $B=-3.0S^{-0.515}$ ;  $\rho_d$  and  $\rho_w$  represent the dry density and the density of liquid water, respectively.

However, the unfrozen water in the frozen fringe is not only affected by the temperature, the equivalent water pressure also plays an important role in determining the unfrozen water content in the frozen fringe. A theory reported by Gilpin (1979) describes the characteristic behavior of water at an ice-water interface, and proposes a pressure near the surface of a solid substrate for driving fluid flow:

$$P = P_0 + P_{Lh} - P_{atm} - \frac{g(h)}{v_w} \quad (20)$$

where the reference pressure  $P_0$  represents the pressure of the reference state in Gilpin's theory (Gilpin, 1979) and denotes the pressure of local bulk water in the unfrozen zone, whereas for the frozen zone, the reference pressure is 1 atm;  $P_{Lh}$  represents the disjoining pressure at the ice-water interface;  $g(\cdot)$  stands for the effect of the solid surface;  $h$  is the thickness of the liquid layer;  $v_w$  is specific volume of the liquid.  $P_{atm}=1$  atm is chosen for both the frozen zone and the unfrozen zone. In the unfrozen zone, the equivalent water pressure  $P$  is the relative pressure of local bulk water, and in the frozen zone the pressure  $P$  is determined by  $P_{Lh}$  and  $h$ . If the water at a specific place is directly connected to the bulk water with the same temperature and reaches an equilibrium state, then the equivalent water pressure at this place equals the pressure of bulk water.

Equating the solid and liquid free energies at the interface, the expression of  $g(h)$  can then be obtained. The pressure, interface, and temperature controlled local thickness of the unfrozen water film is given by the following equation:

$$g(h) = -\Delta v P_{Lh} - v_i \sigma_{iw} \kappa_{iw} - L \frac{T}{T_a} \quad (21)$$

where  $\Delta v = v_i - v_w$ ,  $v_i$  is the specific volume of the ice, and  $L$  is the latent heat.

Substitution of Eq. (20) into Eq. (21) yields:

$$-\Delta v P - v_i \sigma_{iw} \kappa_{iw} - L \frac{T}{T_a} = \frac{v_i}{v_w} g(h) \quad (22)$$

Both temperature and equivalent water pressure have a significant effect on the unfrozen water, as shown in Eq. (22). A variation of  $L/\Delta v T_a$  in equivalent water pressure is equal to 1 °C variation in temperature for the effect on  $h$  and  $\theta_u$ . This means that a pressure difference of 1 MPa is equivalent to a temperature difference of 0.91 °C as far as its potential for impact of unfrozen water. Considering of the equivalent water pressure, the volumetric unfrozen water content (soil freezing characteristic curve) can be rewritten as:

$$\theta_u = \frac{\rho_d}{\rho_w} A \left( -T - \frac{\Delta v T_a}{L} P \right)^B \quad (23)$$

In addition, when Laplace equation is applied and the ice lens growth is regarded as a quasi-static process, the

boundary condition of  $P$  is determined by substitution of Eq. (21) into Eq. (20) and some transformations,  $P=LT/T_a v_w$ .

Eq. (23) accounts explicitly for the equivalent water pressure  $P$ , which is different from Eq. (19). Taking into account both the equivalent water pressure and temperature effects on volumetric unfrozen water content, an equivalent temperature  $T_{eq}$  is introduced in determining the volumetric unfrozen water content:

$$T_{eq} = T + \frac{\Delta v T_a}{L} P \quad (24)$$

Based on the modeling of Eq. (24), it can be found that if the initial temperature varies from  $-0.20^\circ\text{C}$  to  $-0.80^\circ\text{C}$ , the corresponding equivalent temperature varies from  $-0.21^\circ\text{C}$  to  $-0.83^\circ\text{C}$  with considering the effect of equivalent water pressure ( $-100\text{ kPa}$  to  $-300\text{ kPa}$ ) (Fig. 5). Furthermore, the equivalent temperature slowly decreases with decreasing equivalent water pressure. This implies that the equivalent water pressure is necessary to estimate the unfrozen water in frozen fringe. Consequently, the freezing characteristic can be modified as shown in Eq. (25), which accounts explicitly for the equivalent water pressure:

$$\theta_u = \frac{\rho_d}{\rho_w} A (-T_{eq})^B \quad (25)$$

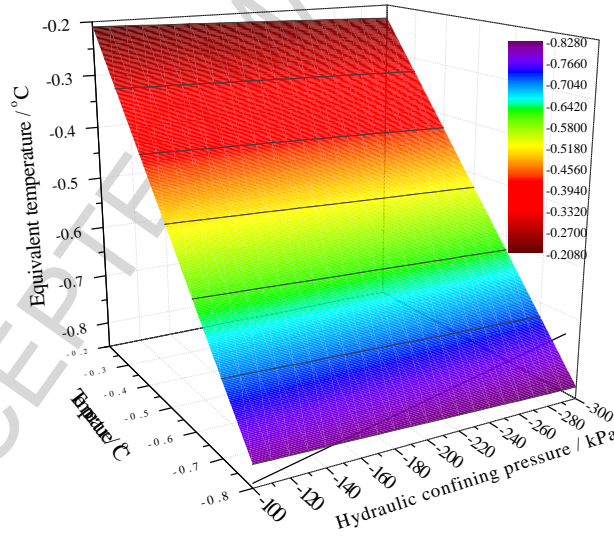


**Fig. 5.** Influence of equivalent water pressure on the equivalent temperature.

The effective porosity and permeability decrease due to the generation of pore ice and the reduction of unfrozen water. Hohenemser and Prager (1932) reported that permeability decreases as effective porosity decreases. Subsequently, He et al. (2018) examined the complete consideration of effective porosity and proved the validity of the equation for fluid flow in freezing soil. This equation is applied to calculate the hydraulic permeability in the frozen fringe, and can be determined as:

$$k_f = k \left( \frac{n_e}{n_0} \right)^5 \left( \frac{1-n_0}{1-n_e} \right)^2 \quad (26)$$

where  $k$  is the initial value of hydraulic permeability;  $n_e$  is the effective porosity which can be replaced by volumetric unfrozen water content  $\theta_w$ ;  $n_0$  is the initial porosity.

### 3.3 Comparison between our new model and the segregation potential model

Following on from the discussion above, Eq. (3) and Eq. (4) comprise the boundary conditions for the calculation of water flow velocity. In addition, Eq. (15), (25) and (26) constitute the primary equations to determine the hydraulic permeability in the frozen fringe. According to the difference of chemical potential along the frozen fringe, the average water permeation flux can then be written as follows:

$$V = \frac{-k_f}{V_{m,w}} \left( \frac{RT_s \ln a_w}{a} + \rho_w g \right) \quad (27)$$

If the basic assumption (i) made in the segregation potential model was employed, the temperature field in the frozen fringe near the thermal steady state is linearly distributed, and can be presented as:

$$\text{grad}T = \frac{T_s - T_f}{a} \quad (28)$$

From these equations, it follows that:

$$\frac{V}{\text{grad}T} = \frac{-(RT_s \ln a_w + \rho_w g a)}{V_{m,w}} k_f \frac{1}{T_s - T_f} \quad (29)$$

In Eq. (29), the first and third terms on the right-hand side are determined by the segregation temperature, and the second term on the right-hand side of Eq. (29) is the hydraulic permeability in the frozen fringe. If the basic assumption (ii) made in the segregation potential model is applied, then Eq. (29) can be considered as a constant. Also, the constant can be regarded as a mathematical description of segregation potential.

The derivation above shows that the quasi-static model developed in this paper can be transformed to the segregation potential model if the two basic assumptions made in the segregation potential model are applied. Hence, our new model can be regarded as an extension of the segregation potential model. The segregation temperature in the segregation potential model is considered as a constant value during the calculation of water flow velocity. However, our new model enables the calculation of the ice lens growth under a slowly varying segregation temperature, and hence, it describes the quasi-static process for frost heave.

## 4 Numerical simulation and model validation

### 4.1 Test and calculation conditions

Based on one-dimensional freezing experiments of saturated silty clay, we have conducted the numerical simulation applying the water activity based quasi-static model developed in this paper with calculations carried out

using MATLAB R2017a. Validation of the new model is demonstrated through comparison of the predicted results with the experimental measurements. Zhou et al. (2006) conducted the freezing tests with samples having a dry unit weight of  $1.48 \text{ g/cm}^3$  and size of 13 cm high and 10.1 cm in diameter. The mass fraction of clay in the soil is 32.45% and that of silt is 67.15%. The cold and warm end temperature is  $-12 \text{ }^\circ\text{C}$  and  $6 \text{ }^\circ\text{C}$ , respectively. The saturated water content of the tested soil is 0.30. In the freezing tests, the infrared radiation method was applied to measure the temperature of the ice lens. The temperature of the warmest ice lens varied with time during freezing (Fig. 6), inducing corresponding variation of the driving force and the hydraulic permeability for the capillary flow in the frozen fringe.

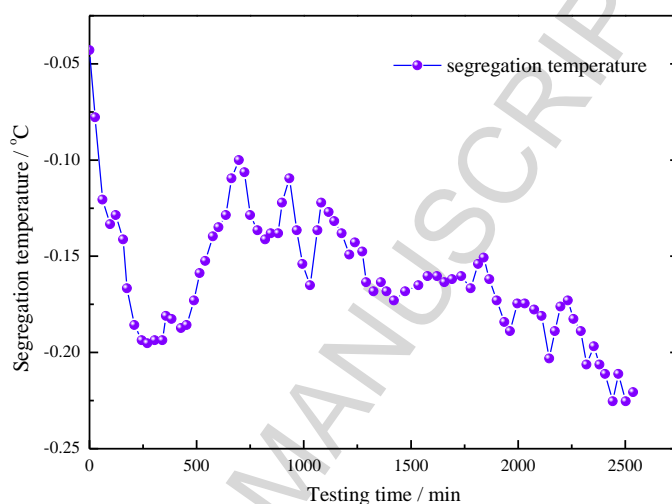


**Fig. 6.** Result of the segregation temperature of the warmest ice lens.

In addition, the main material parameters for numerical calculation are listed in Table 1.

**Table 1** The main parameters for the computational model.

Parameters	Unit	Value
$\rho_w$	$\text{kg/m}^3$	1000
$\rho_i$	$\text{kg/m}^3$	900
$L$	$\text{kJ/kg}$	334.56
$\Delta_m H_1(T_f)$	$\text{J/mol}$	6010
$\Delta C_p$	$\text{J/K mol}$	38.2
$R$	$\text{J/K mol}$	8.314
$V_{m,w}$	$\text{m}^3/\text{mol}$	$1.8 \times 10^{-5}$

The numerical simulation was conducted based on the experiment, and the same conditions were applied to verify the applicability of the new quasi-static model.

## 4.2 Results and analyses

By substituting the segregation temperature (shown in Fig. 6) into the boundary condition Eq. (4), the numerical simulations of hydraulic permeability, water activity, and ice lens growth (frost heave) can then be carried out. Ice crystals are gradually generated with decreasing water activity, inhibiting fluid flow in porous media. In order to analyze the effect of water activity on the hydraulic permeability, the temperature is generally distinguished into two stages, termed the Cooling Stage (I) and Warming Stage (II) (shown in Fig. 7). When the temperature  $T=T_f$ , and ice and

water coexist in equilibrium in the soil. When  $T < T_f$ ,  $a_w < 1$ , water freezes to ice crystals. In the Cooling Stage (I), water activity decreases with temperature, favoring the formation of ice crystals. Ice crystals are gradually formed as the water activity decreases, resulting in the increase of the volumetric ice content and the decrease of fluid conduits (effective porosity). Hence, the hydraulic permeability in the frozen fringe significantly decreases with the decrease of water activity (Fig. 7). This correlation is a consequence of the formation of pore ice in the frozen fringe, leading to a decrease in hydraulic permeability due to pore blocking. In the Warming Stage (II), an opposite trend is observed, whereby the hydraulic permeability increases as the water activity increases. In this stage, some ice crystals melt gradually to water, providing more seepage pathways and facilitating fluid flow. Correspondingly, the hydraulic permeability increases. Hence, improvement in the theory of temperature- and equivalent water pressure-dependent hydraulic permeability in our model (section 3.2.2) does not only provide a calculation for flow challenges, but it also provides new insights into the physical mechanism that underlies pore blocking and related phenomena.

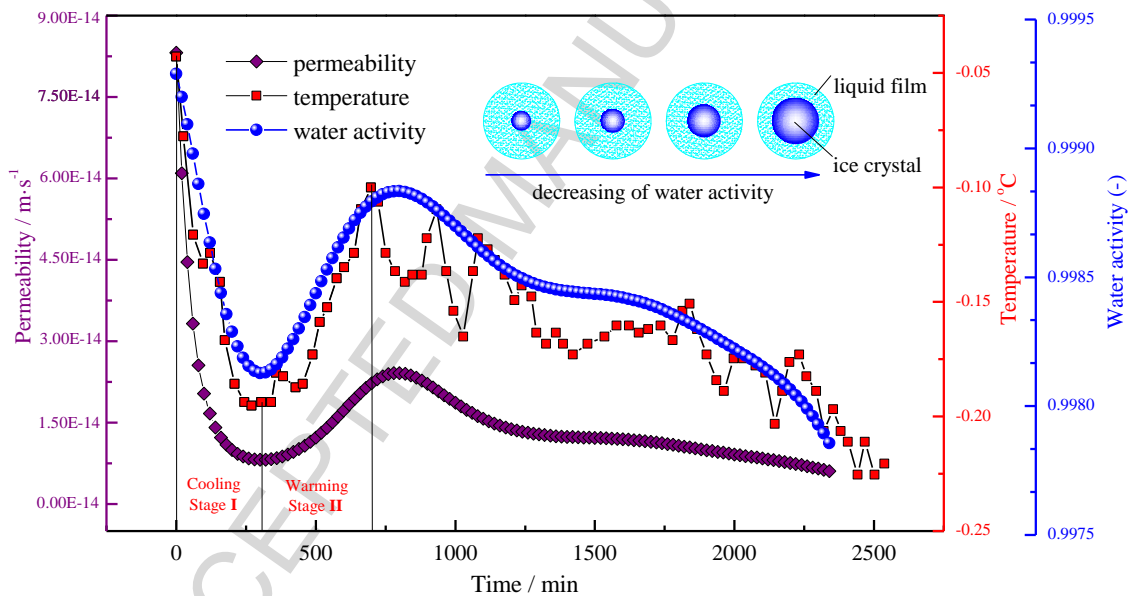


Fig. 7. Result of hydraulic permeability in the frozen fringe.

Using the hydraulic permeability result, the water activity based numerical simulation of the ice lens growth is carried out, and we refer to this calculated result as ‘Frost heave-I’. There is a generally good agreement between the numerical model and the experimental result (Fig. 8). Moreover, the numerical result of the ice lens growth (Frost heave-I) is slightly larger than the experimentally measured result at the onset of test at Stage I (Fig. 8). It is interpreted that a relatively high temperature of the ice lens (as shown in Fig. 7) at the onset of the test causes a relatively high calculated permeability in the freezing soil. Similarly, the water flow velocity is larger under this condition, which in turn results in a rapid growth of the ice lens at this stage. Furthermore, the relatively low temperature of the ice lens in the Stage II significantly decreases the water flow velocity due to the relatively low permeability caused by pore

blocking. Hence, the rate of the growth of the ice lens slows down at this stage. Such fast variation of temperature of the ice lens causes a slight difference between the measured and calculated ice lens growth in Stage I and II. However, the calculated result of the ice lens growth agrees very well with the measured result after 800 minutes. The disparity between the ultimate experimental observation (6.40 mm) and the Frost heave-I (6.12mm) is 4.38%.

Moreover, using the same soil parameters, the conventional pressure potential gradient (Eq. 24) in Darcy's law is introduced into our new model as the driving force to calculate the ice lens growth, and this result is referred to as 'Frost heave-II'. Both patterns of ice lens growth under the conditions of Frost heave-I and II present a similar trend (Fig. 8). The disparity between the ultimate experimental observation and the Frost heave-II (5.86 mm) is 8.46%. Comparison between the result of Frost heave-I and II shows that the Frost heave-I based on our new developed model matches the experimental results significantly better, especially for the data after 800 minutes (Fig. 8). Thus, although the pressure gradient based calculation offers a good prediction of the ice lens growth (Frost heave-II), the result of Frost heave-I is much closer to the experimental observation.

In order to compare the results of frost heave under constant and variable segregation temperatures, the average value of the segregation temperature is substituted into the boundary condition Eq. (4), a water activity based simulation of the growth of the ice lens is then carried out, and we refer to this calculated result as 'Frost heave-III' (Fig. 8). The pattern of ice lens growth (linear growth) under the condition of Frost heave-III presents a different trend to the experimental observation since the segregation temperature is a constant value. Furthermore, the disparity between Frost heave-III (5.26 mm) and the ultimate experimental observation increases to 17.83%. We can thus conclude that, the good agreement between the calculated result (Frost heave-I) and the experimental observation verifies the new model presented in this paper.

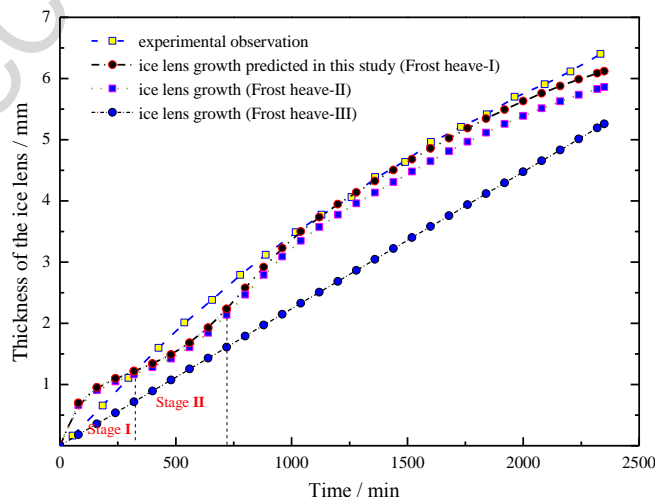


**Fig. 8.** Comparison of thickness of the ice lens between the observation and calculation.

The analysis above showed that the water activity based model is capable of describing the growth of the ice lens,

and can be employed to simulate frost heave. In addition, this study improves our understanding of the physical mechanisms that underlie ice nucleation, fluid flow in partially frozen granular media and related phenomena, and provides a new method to predict frost heave at a quasi-static state.

#### 4 Conclusions

(1) A quasi-static model for the growth of an ice lens is proposed in this paper by considering the limitation of the segregation potential model. A water activity based chemical potential gradient in this paper replaces the conventional pressure potential gradient in Darcy's law for the calculation of water flow velocity. Moreover, a mathematical description of the empirical constant of the segregation potential is provided after the analysis of the new developed model. Our model enables the calculation of the ice lens growth under a slowly varying segregation temperature, which can be considered as an extension of the segregation potential model.

(2) The modified Kozeny-Carman equation is used to describe the water permeability of a given soil. However, the presence of the pore ice in the frozen fringe results in the decrease of the hydraulic permeability due to pore blocking. In this paper, the effect of pore water pressure is taken into account to modify the freezing characteristic function, and to determine the unfrozen water content in the frozen fringe. Subsequently, the temperature- and pressure-dependent hydraulic permeability in the frozen fringe is then mathematically determined and improved.

(3) The water activity based model provides a quantitative method to describe the state of water at a specific temperature, and offers a new method to predict frost heave after the active zone reaches a thermal steady state. The good agreement between the calculated result and experimental observation verifies our new model. In this paper, we focus on the description of the growth of the ice lens, whereas theoretical developments of the formation mechanism of ice lenses involve molecular scale chemical physics and still require further research studies. The theoretical study in this paper can be used as a foundation for further theoretical and experimental developments and to gain more insight into the intriguing geophysical phenomenon of frost heave.

#### Acknowledgments

This research was supported by Outstanding Innovation Scholarship for Doctoral Candidate of "Double First Rate" Construction Disciplines of CUMT.

#### References

- [1] Anderson, D.M., Tice, A.C., 1972. Predicting unfrozen water contents in frozen soils from surface area measurements. *Highw. Res. Rec.* 393, 12-18.

- [2] Akagawa, S., 1988. Experimental study of frozen fringe characteristic. *Cold. Reg. Sci. Technol.* 15(3), 209-223.
- [3] Carman, P.C., 1937. Fluid flow through a granular bed. *Trans. Inst. Chem. Engrs.* 15, 150-156.
- [4] Dash, J.G., Fu, H.Y., Wettlaufer, J.S., 1995. The premelting of ice and its environmental consequences. *Rep. Prog. Phys.* 58(1), 115-167.
- [5] Fremond, M., Mikkola, M., 1991. Thermomechanical modeling of freezing soil, in: *Proceedings of 6th International Symposium on Ground Freezing*. pp, 17-24.
- [6] Gilpin, R.R., 1979. A model of the "liquid-like" layer between ice and a substrate with applications to wire regelation and particle migration. *J. Colloid. Interf. Sci.* 68 (2), 235-251.
- [7] Gilpin, R.R., 1980. A model for the prediction of ice lensing and frost heave in soils. *Water. Resour. Res.* 16 (5), 918-930.
- [8] Hohenemser, V.K., Prager, W., 1932. Über Die ansätze der mechanik isotroper kontinua. *J. Appl. Math. Mech.* 12 (4), 216-226.
- [9] Harlan, R.L., 1973. Analysis of coupled heat-fluid transport in partially frozen soil. *Water. Resour. Res.* 9 (5), 1314-1323.
- [10] He, Z.Y., Zhang, S., Teng, J.D., Yao, Y.P., Sheng, D.C., 2018. A coupled model for liquid water-vapor-heat migration in freezing soils. *Cold Reg. Sci. Technol.* 148, 22-28.
- [11] Ji, Y.K., Zhou, G.Q., Zhao, X.D., Wang, J.Z., Wang, T., Lai, Z.J., Mo, P.Q., 2017. On the frost heaving-induced pressure response and its dropping power-law behaviors of freezing soils under various restraints. *Cold Reg. Sci. Technol.* 142, 25-33.
- [12] Ji, Y.K., Zhou, G.Q., Zhou, Y., Matthew, R.H., Zhao, X.D., Mo, P.Q., 2018. A separate-ice based solution for frost heaving-induced pressure during coupled thermal-hydro-mechanical processes in freezing soils. *Cold Reg. Sci. Technol.* 147, 22-33.
- [13] Kozeny, J., 1927. Über kapillare Leitung des Wasser im Boden. *Sitzungsber. Akad. Wiss. Wien.* 136, 271-306.
- [14] Konrad, J.M., Morgenstern, N.R., 1980. A mechanistic theory of ice lens formation in fine-grained soils. *Can. Geotech. J.* 17, 473-486.
- [15] Konrad, J.M., Morgenstern, N.R., 1981. The segregation potential of a freezing soil. *Can. Geotech. J.* 18(4), 482-491.
- [16] Konrad, J.M., Morgenstern, N.R., 1982. Effects of applied pressure on freezing soils. *Can. Geotech. J.* 19 (4), 494-505.
- [17] Konrad, J.M., Shen, M., 1996. 2-D frost action modeling using the segregation potential of soils. *Cold Reg. Sci. Technol.* 24(3), 263-278.
- [18] Koop, T., Luo, B.P., Tsias, A., Peter, T., 2000. Water activity as the determinant for homogeneous ice nucleation in aqueous solutions. *Nature* 406, 611-614.
- [19] Loch, J.P.G., Miller, R D., 1975. Test of the concept of secondary frost heaving. *Soil Sci. Soc. Am. J.* 39(6), 1036-1041.
- [20] Lai, Y.M., Pei, W.S., Zhang, M.Y., Zhou, J.Z., 2014. Study on theory model of hydro-thermal-mechanical interaction process in saturated freezing silty soil. *Int. J. Heat Mass Transf.* 78, 805-819.
- [21] Lai, Y.M., Wu, D.Y., Zhang, M.Y., 2017. Crystallization deformation of a saline soil during freezing and thawing processes. *Appl. Therm. Eng.* 120, 463-473.
- [22] Li, A.Y., Niu, F.J., Zheng, H., Akagawa, S., Lin, Z.J., Luo, J., 2017. Experimental measurement and numerical simulation of frost heave in saturated coarse-grained soil. *Cold Reg. Sci. Technol.* 137, 68-74.
- [23] Michalowski, R.L., Zhu, M., 2006. Frost heave modelling using porosity rate function. *Int. J. Numer. Anal. Meth. Geomech.* 30, 703-722.
- [24] Nixon, J.F., 1982. Field frost heave predictions using the segregation potential concept. *Can. Geotech. J.* 19(4), 526-529.
- [25] Nixon, J.F., 1991. Discrete ice lens theory for frost heave in soil. *Can. Geotech. J.* 28 (6), 843-859.

- [26] O'Neil, K., Miller, R.D., 1985. Exploration of a rigid ice model of frost heave. *Water. Resour. Res.* 21 (3), 281-296.
- [27] Palmer, A.C., Williams, P.J., 2003. Frost heave and pipeline upheaval buckling. *Can. Geotech. J.* 40(5), 1033-1038.
- [28] Roque, A.J., Didier, G., 2006. Calculating hydraulic conductivity of fine-grained soils to leachates using linear expressions. *Eng. Geol.* 85, 147-157.
- [29] Rempel, A.W., Wettlaufer, J.S., Worster, M.G., 2004. Premelting dynamics in a continuum model of frost heave. *J. Fluid. Mech.* 498: 227-244.
- [30] Rempel, A.W., 2007. Formation of ice lenses and frost heave. *J. Geophys. Res.* 112, F02S21.
- [31] Ren, X.W., Zhao, Y., Deng, Q.L., Kang, J.Y., Li, D.X., Wang, D.B., 2016. A relation of hydraulic conductivity-void ratio for soils based on Kozeny-Carman equation. *Eng. Geol.* 213, 89-97.
- [32] Scherer, G.W., 1999. Crystallization in pores. *Cement Concrete Res.* 29, 1347-1358.
- [33] Sheng, D.C., Zhang, S., Yu, Z.W., Zhang, J.S., 2013. Assessing frost susceptibility of soils using PCHeave. *Cold Reg. Sci. Technol.* 95 (11), 27-38.
- [34] Sun, M.L., 2014. Analysis of the specific surface area of loess in Lanzhou. MSc Thesis (In Chinese). Lanzhou University, Lan Zhou, China.
- [35] Sante, M.D., Fratolocchi, E., Mazzieri, F., Brianzoni, V., 2015. Influence of delayed compaction on the compressibility and hydraulic conductivity of soil-lime mixtures. *Eng. Geol.* 185, 131-138.
- [36] Sizemore, H.G., Zent, A.P., Rempel, A.W., 2015. Initiation and growth of martian ice lenses. *Icarus* 251, 191-210.
- [37] Tarnawski, V.R., Wagner, B., 1996. On the prediction of hydraulic conductivity of frozen soils. *Can. Geotech. J.* 33, 176-180.
- [38] Tiedje, E.W., Guo, P.J., 2012. Frost heave modeling using a modified segregation potential approach. *J. Cold Reg. Eng.* 686-696.
- [39] Woster, M.G., Wettlaufer, J.S., 1999. The fluid mechanics of premelted liquid films. In: Shyy, W., Narayanan, R. (Eds.), *Fluid Dynamics of Interface*. Cambridge University Press, pp. 339-351.
- [40] Wu, D.Y., Lai, Y.M., Zhang, M.Y., 2015. Heat and mass transfer effects of ice growth mechanisms in a fully saturated soil. *Int. J. Heat Mass Transf.* 86, 699-709.
- [41] Zhou, J.S., Zhou, G.Q., Ma, W., Wang, J.Z., Zhou, Y., Ji, S.B., 2006. Experimental research on controlling frost heave of artificial frozen soil with intermission freezing method. *Journal of China University of Mining and Technology* 35(6), 708-712 (In Chinese).
- [42] Zobrist, B., Marcolli, C., Peter, T., Koop, T., 2008. Heterogeneous ice nucleation in aqueous solutions: the role of water activity. *J. Phys. Chem. A* 112, 3965-3975.
- [43] Zhou, Y., Zhou, G.Q., 2012. Intermittent freezing mode to reduce frost heave in freezing soils-experiments and mechanism analysis. *Can. Geotech. J.* 49 (6), 686-693.
- [44] Zhou, J.Z., Li, D.Q., 2012. Numerical analysis of coupled water, heat and stress in saturated freezing soil. *Cold Reg. Sci. Technol.* 72, 43-49.
- [45] Zhang, S., Sheng, D.C., Zhao, G.T., Niu, F.J., He, Z.Y., 2014. Analysis of frost heave mechanisms in a high-speed railway embankment. *Can. Geotech. J.* 53(3), 520-529.
- [46] Zhang, M., Wen, Z., Xue, K., Chen, L., Li, D., 2016. A coupled model for liquid water, water vapor and heat transport of saturated-unsaturated soil in cold regions: model formulation and verification. *Environ. Earth. Sci.* 75 (8), 701.

## List of Figures

**Fig. 1.** Schematic of soil column after the appearance of the warmest ice lens.

**Fig. 2.** The relationship between hydraulic permeability and specific surface area (void ratio=0.4).

**Fig. 3.** The specific surface area of different soil types.

**Fig. 4.** Schematic diagram of the frozen fringe.

**Fig. 5.** Influence of equivalent water pressure on the equivalent temperature.

**Fig. 6.** Result of the segregation temperature of the warmest ice lens.

**Fig. 7.** Result of hydraulic permeability in the frozen fringe.

**Fig. 8.** Comparison of thickness of the ice lens between the observation and calculation.

## List of Tables

**Table 1** The main parameters for the computational model.

**Table 1** The main parameters for the computational model.

Parameters	Unit	Value
$\rho_w$	kg/m <sup>3</sup>	1000
$\rho_i$	kg/m <sup>3</sup>	900
$L$	kJ/kg	334.56
$\Delta_m H_1(T_f)$	J/mol	6010
$\Delta C_p$	J/K mol	38.2
$R$	J/K mol	8.314
$V_{m,w}$	m <sup>3</sup> /mol	$1.8 \times 10^{-5}$

**Highlights**

A new quasi-static model for ice lens growth under a time varying temperature is established based on the water activity criterion.

A mathematical description of the segregation potential is provided based on the analysis of the new developed model.

The temperature- and pressure- dependent hydraulic permeability in the frozen fringe is mathematically determined and improved.

ACCEPTED MANUSCRIPT